Design Considerations for an Infrared Imaging Video Bolometer for Observation of 3D Radiation Structures of Detached LHD Plasmas*)

Shwetang N. PANDYA and Byron J. PETERSON[1)]

The Graduate University for Advance Studies, 322-6 Oroshi-cho, Toki 509-5292, Japan
[1)]*National Institute for Fusion Science, 322-6 Oroshi-cho, Toki 509-5292, Japan*

(Received 9 December 2011 / Accepted 17 May 2012)

Infrared Imaging Video Bolometers (IRVBs) are successfully being used to study the three dimensional impurity radiation distribution from the LHD plasma. IRVBs can serve as a promising diagnostic for studying the radiation structures of detached plasmas in LHD and hence a comparison can be established with theoretical models. A new IRVB system is being designed for the LHD bottom port for better access to the magnetic x-points and to study the 3D radiation structures. The design overview of this new IRVB system is discussed in this paper. The design includes spatial resolution, field of view of the IRVB, sensitivity and signal to noise estimates. Two optical configurations for an infrared periscope are discussed in brief and selection of a catadioptic configuration with a cassegrain telescope is justified. The sensitivity of the existing IRVBs is expected to increase 5 fold by the addition of this IR periscope.

Keywords: infrared imaging video bolometer, plasma detachment, divertor power load, 3D radiation structure, IRVB design, LHD plasma

DOI: 10.1585/pfr.7.2402095

1. Introduction

The pursuit for pushing the machine parameters towards high power operation tends to approach the design limits of the plasma facing components (PFCs). This endangers the integrity and hence the lifecycle of the PFCs to an extent that can lead to a sudden failure. Measures to keep the power loads on the PFCs within the engineering design limits need to be practiced to enhance the lifespan and proper functionality of the PFCs. Among several schemes under consideration, detachment of plasma from the PFCs is a promising candidate. Plasma detachment will reduce the power load on the PFCs by enhancing the radiation from the plasma. It is a well known fact that the radiation emitted by the plasmas in a broad wavelength spectrum can be very well studied by bolometers. The infrared imaging video bolometer (IRVB) has an advantage of measuring the plasma radiation in two dimensions. The radiation structures emerging during the detachment of plasmas can be studied by the IRVB. This paper describes various design parameters for one such IRVB module planned to be installed on the bottom port for viewing radiative structures during detachment experiments on LHD. Section 2 describes the detachment process and localization of radiation structures. Section 3 gives an explanation about the IRVB and discussion on various design parameters. IRVB sensitivity and its dependence on camera performance are discussed in Section 4. In Section 5 a brief discussion is given about the optics being planned for the new IRVB. Conclusions are given in Section 6.

2. Magnetic Islands & Plasma Detachment

Plasma detachment is an important operational regime for future diverted magnetic fusion devices. Detachment in a tokamak is achieved by raising the plasma density to the density threshold. But LHD plasma terminates due to radiative collapse even before the density threshold is reached [1]. Hence, plasma detachment in LHD is aided by the external addition of an $m/n = 1/1$ magnetic island (MI) perturbation [2]. The MI is introduced in the stochastic region with the help of saddle perturbation field coils. Addition of the MI lowers the density threshold and helps in achieving sustained detachment [2]. The radiation structures are found to be localized near the magnetic islands x-points (MIXs) with detachment and near the helical diverter x-points (HDXs) without detachment [2,3] in the presence of the MI. This radiative localization is also shown by EMC3-EIRENE edge transport models [4,5]. A synthetic diagnostic code is used to integrate the 3D radiation intensity distribution given by the EMC3-EIRENE code, through the field of view (FOV) of each detector of the IRVB. This exercise will generate a two-dimensional image of the radiation structures which can easily be com-

author's e-mail: pandya.shwetang@LHD.nifs.ac.jp

*) This article is based on the presentation at the 21st International Toki Conference (ITC21).

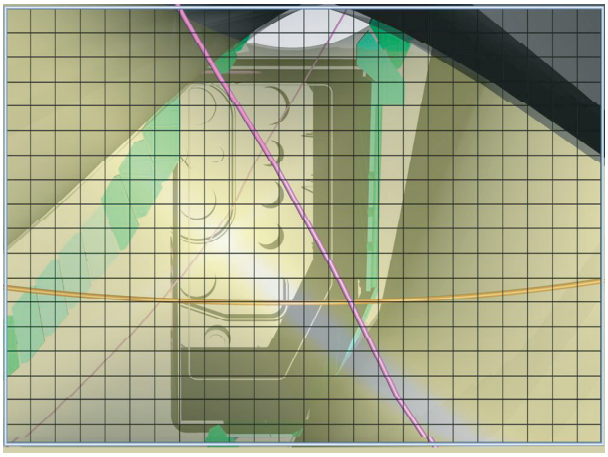

Fig. 1 CAD of the bottom view of the imaging bolometer. The grid shows the subdivision of the IRVB field of view into individual channels. The brown line indicates the magnetic axis and the pink line indicates the location of helical divertor x-point.

pared with the experimental data obtained from the IRVB [6]. Adding IRVB FOVs provides more information on the radiation patterns from plasmas. Hence it is decided to add an IRVB at the bottom port of LHD for having better access to the radiation structures. This will also help in establishing a comparison with other IRVB views. The design of this IRVB is discussed in the succeeding section.

3. Infrared Imaging Video Bolometer

IRVBs have been successfully employed on LHD since a decade for estimation of radiated power from the plasmas. The estimation of total radiated power in tokamaks can be made by measuring the power emitted from one poloidal cross-section using a linear detector array, assuming toroidal symmetry. Since LHD has a three-dimensional geometry it is helpful to measure the radiated power in two dimensions. The IRVB gives the capability for such measurements in two dimensions, along with other flexibilities over conventional bolometer systems. The IRVB module consists of an aperture plate, a light shielding tube, a thin metal foil sandwiched between two copper masks, an IR vacuum window and an IR camera [7]. The foil will work as an absorber for the radiation emitted by the plasma and on the other side the IR camera will measure the radiation emitted by the heated foil. The IR camera is placed inside a soft iron magnetic shield so that it is not affected by the high field produced by the LHD magnets. Figure 1 shows the IRVB FOV from the bottom port.

The power emitted from the LHD plasma can be estimated by solving the 2D heat diffusion equation given by Eq. (1) in terms of the radiated power P_{rad} [8].

$$-\Omega_{\mathrm{rad}} + \Omega_{\mathrm{bb}} + \frac{1}{\kappa}\frac{\partial T}{\partial t} = \frac{\partial^2 T}{\partial x^2} + \frac{\partial^2 T}{\partial y^2} \qquad (1)$$

where

$$\Omega_{\mathrm{bb}} = \frac{\varepsilon\sigma_{\mathrm{S\text{-}B}}(T^4 - T_0^4)}{kt_{\mathrm{f}}}$$

and

$$\Omega_{\mathrm{rad}} = \frac{P_{\mathrm{rad}}}{kt_{\mathrm{f}}l^2}$$

Where t_{f}, k and κ are thickness, thermal conductivity and thermal diffusivity of the foil respectively. T is the temperature, x and y are the spatial coordinates of the IRVB pixel of area l^2 and t is the time. $\sigma_{\mathrm{S\text{-}B}}$ is the Stephen-Boltzmann constant and ε is the emissivity. Calibration for the IRVB foil [9] has to be done in order to determine the unknown parameters kt_{f}, ε and κ where ε is the emissivity of the graphite spray used to increase the radiation from the thin metal foil on the IR camera side. These parameters need to be estimated for each pixel of the IRVB foil. The selection of the foil material plays an important role in the performance of the IRVB. The upper and lower threshold of the absorbed photon energy by the material determines the wavelength bandwidth of the IRVB. The material should have a wide absorption bandwidth.

The noise equivalent power and hence the sensitivity of the IRVB significantly depend on the selection of the foil material. The noise equivalent power for an IRVB [9] is given by Eq. (2)

$$\eta_{\mathrm{IB}} = \frac{\sqrt{10}kt_{\mathrm{f}}\sigma_{\mathrm{IR}}}{\sqrt{mN}}\sqrt{1 + \frac{l^4}{5\kappa^2 m^2 \Delta t_{\mathrm{IR}}^2} + \frac{4l^4\varepsilon^2\sigma_{\mathrm{S\text{-}B}}^2 T^6}{5k^2 t_{\mathrm{f}}^2}} \qquad (2)$$

Assuming the first and third term under the square root to be negligible for temperatures less than 1000°C Eq. (2) can be rewritten as follows.

$$\eta_{\mathrm{IB}} \cong \frac{\sqrt{2}kt_{\mathrm{f}}\sigma_{\mathrm{IR}}l^2}{\Delta t_{\mathrm{IR}}\kappa\sqrt{m^3N}} \propto kt_{\mathrm{f}}/\kappa \propto 1/\text{Bolometer Sensitivity} \qquad (3)$$

From Eq. (3) it is clear that bolometer sensitivity is proportional to κ/k, both of which are material properties. Although the κ/k ratio for Platinum (Pt) is lower than Gold (Au), it is experimentally confirmed that the Pt foil is 9 times more sensitive than Au foil [10]. The neutron cross-sections should also be considered for the selection of foil material since neutrons are expected from D-D experiments on LHD in the near future. The best candidate with the lowest neutron cross-section is Pt [11]. Hence platinum seems to be an appropriate candidate for the foil material with the smallest neutron cross section, broader energy absorption bandwidth and better sensitivity.

The typical foil dimension will be 13 cm × 10 cm (horizontal × vertical) and the foil thickness will be 2.5 μm which can absorb photon energies upto 8.2 keV [11]. The resulting IRVB configuration will have 24 × 18 channels (horizontal × vertical) considering an aperture 8 mm × 8 mm in size. The spatial resolution at the plasma mid-plane is expected to be 5.2 cm with a 432 channel IRVB module. FOV of the IRVB will be 32° × 24° so as to have full coverage of the plasma mid-plane.

Table 1 Performance parameters of IR cameras and the resulting S_{IRVB} for a platinum IRVB foil with N_{bol} = 432, A_f = 130 cm^2, t_f = 2.5 μm, f_{bol} = 30 Hz (S - Sterling, μbolo - microbolometer).

Maker/ IR Camera	FLIR/ Omega	FLIR/ SC 500	FLIR/ SC 655	FLIR/ SC 4000	FLIR/ SC 8000
λ(μm)	7.5-13.5	7.5-13	7.5-13	3-5	3-5
S_{IR} (mºC @30ºC)	100	100	50	25	25
type	μbolo	μbolo	μbolo	InSb	InSb
cooling style	none	none	none	S	S
N_{IR}	160 × 120	320 × 240	640 × 480	320 × 256	1024 × 1024
f_{IR} (Hz)	30	60	50	420	132
S_{IRVB} (μW/cm^2)	455	161	44	14	7

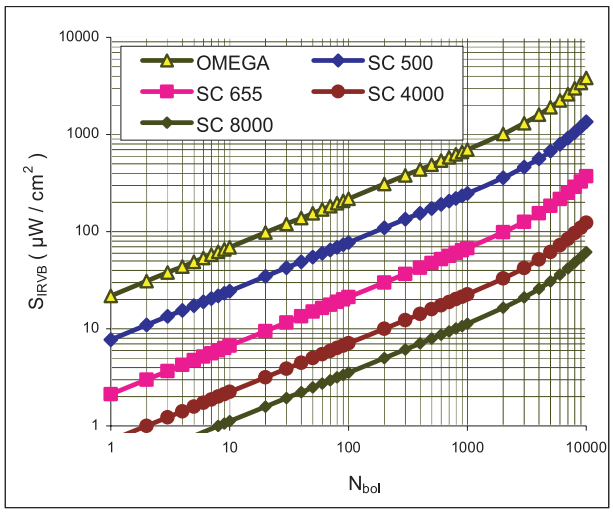

Fig. 2 S_{IRVB} versus N_{bol} for a platinum IRVB foil with A_f = 130 cm^2, t_f = 2.5 μm, f_{bol} = 30 Hz for 5 different IR cameras.

4. Camera Performances and Sensitivity

The noise equivalent power density (NEPD) is the figure of merit for an IRVB and can be written by dividing the noise equivalent power given by Eq. (1) by the bolometer pixel area [9] as given by Eq. (4).

$$S_{IRVB} = \frac{\eta_{IRVB} N_{bol}}{A_f} = \frac{\sqrt{10} k t_f \sigma_{IR}}{\sqrt{f_{IR} N_{IR}}} \sqrt{\frac{N_{bol}^3 f_{bol}}{A_f^2} + \frac{N_{bol} f_{bol}^3}{5\kappa^2}} \quad (4)$$

Eq. (4) is derived in terms of the sensitivity of the IR camera σ_{IR}, operating at a frame rate of f_{IR} and having N_{IR} pixels. Frame rate, f_{bol}, and number of channels, N_{bol}, are the IRVB parameters and A_f is the area of the foil. Table 1 shows the variation in IRVB NEPD with the performance parameters of the IR cameras. Figure 2 plots the IRVB NEPD versus the number of bolometer pixels. It is clear from Table 1 and Fig. 2 that the sensitivity of the IRVB can be improved by using a high performance IR camera. NEPD calculations in Table 1 and Fig. 2 are done considering a 2.5 μm platinum foil. Considering a tradeoff between the IRVB sensitivity and the cost effectiveness of the IR camera it has been decided to select an FLIR SC655 camera for the new IRVB at the bottom port.

5. Optics Design

The infrared camera is the heart of the IRVB system. It is very sensitive to the high magnetic field produced by the LHD superconducting coils and also vulnerable to the high energetic neutrons produced during the future D-D experiments on LHD. Hence designing infrared periscope optics will have two clear advantages for this new IRVB at a bottom port namely shielding the camera from the high magnetic field and highly energetic neutrons and increased sensitivity of the IRVB. Figure 3 shows the CAD schematic for the IRVB module for the bottom port. Three possible locations L1, L2 and L3 at 2700, 4700 and 6700 mm from the IRVB foil respectively are being considered for placing the camera. Location L1 is most susceptible to high magnetic field and neutrons. Location L2 is far from the LHD coil hence neutron bombardment is the only threat, whereas location L3 is the safest location to place the camera since it has a 2000 mm concrete slab which acts as a neutron shield. For the upcoming experimental campaign of LHD location L1 would be best for mounting the camera since there are no D-D experiments for the time being and hence no neutrons. Also SC655 is a micro-bolometer camera which does not have a Sterling cooler and hence no motorized parts which can be affected by a high magnetic field. The SC655 is equipped with a 15° × 11° FOV lens.

It is a known fact that the spatial resolution deteriorates with increasing distance between the IRVB foil and the camera since the FOV of the IR camera expands with distance. The instantaneous FOV of a 15° × 11° lens at 2700 mm is 1.11 mm^2 which corresponds to 117 × 90 pixels of IR camera actually imaging the foil. But from Table 1 it is clear that the IRVB NEPD, S_{IRVB}, decreases (improves) with the number of IR camera pixels, N_{IR}, imaging the IRVB foil. This fact calls for the design of appropriate infrared optics that can allow increasing the distance between the camera and the IRVB foil while maintaining good spatial resolution. The S_{IRVB} calculated for the 15° × 11° lens would turn out to be 240 μW/cm^2 considering 117 × 90 camera pixels imaging the foil. The infrared optics being designed will image the foil with 640 × 480 pixels such that S_{IRVB} would approach the theoretical minimum (assuming the FOV matching the foil size) of 44 μW/cm^2 for the SC655 camera. The addition of infrared optics would thus result in a 5.45 fold increase in the sensitivity of the IRVB system.

The infrared optics being designed need to have good

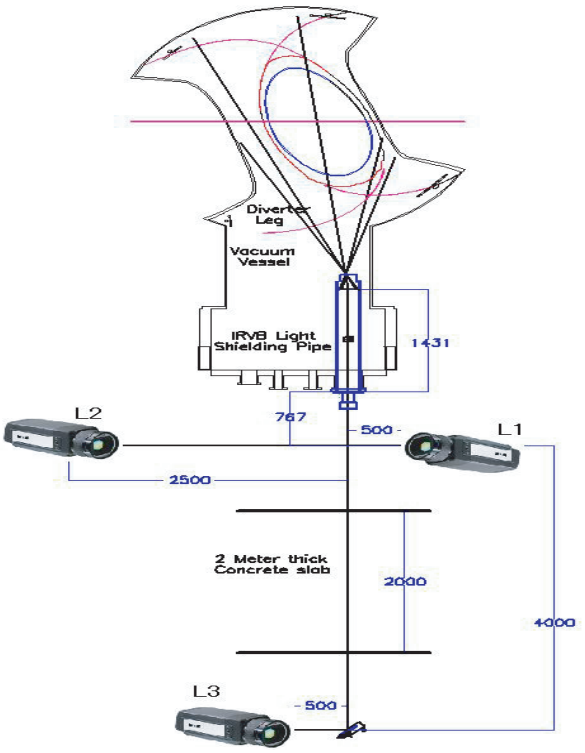

Fig. 3 CAD schematic for IRVB assembly at lower port on LHD.

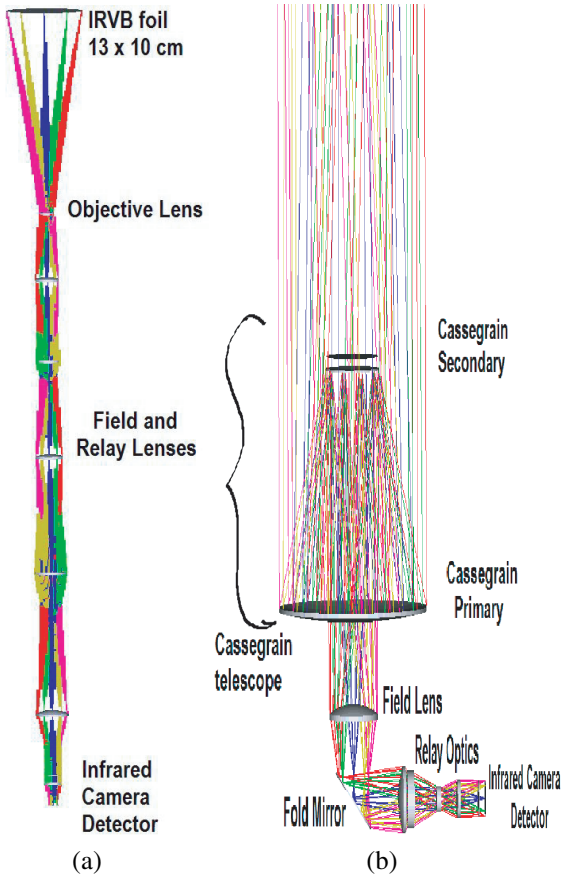

Fig. 4 (a) the refractive optics configuration and (b) the catadioptric cassegrain configuration for location L1.

optical throughput and should be able to withstand the neutron irradiation during future D-D experiments on LHD. Two optical configurations are being compared for this optics design. The first configuration is a refractive design consisting of several lenses. The second is a catadioptric configuration which can be designed by using a reflective cassegrain telescope [12] and a few lenses for focusing the image on the infrared camera detector. The refractive optics are vulnerable to neutron irradiation which may change their optical properties and hence transmission [13], whereas the reflective mirrors can withstand neutron bombardment for a longer period. Refractive optics can not be made bigger in size. This will increase the manufacturing cost and also bigger refractive optical elements are prone to deformation due to their own weight. On the other hand the reflective mirrors can be made lighter and bigger in size. The total throughput of the refractive assembly made up of 6 to 7 lens each having a transmission $\sim 85\%$ would turn out to be less than 35%. Since the temperature rise of the foil is hardly a few degrees this transmission loss can not be tolerated. The reflective cassegrain configuration on the other hand can be designed with two mirrors, each having a reflection $> 95\%$ and a few lens elements having a transmission $\sim 85\%$ would result in a system having a throughput $> 65\%$. The sensitivity of the IRVB is directly proportional to the transmission throughput of the optics [14]. The use of a reflective cassegrain configuration would result in an 85% more sensitive IRVB as compared to the refractive counterpart. Refractive optics have both spherical and chromatic aberrations, hence more lens elements are needed to correct these aberrations which in turn will reduce the throughput of the optics. Whereas the reflective optics are free from both these aberrations. Considering the above mentioned aspects and merits of a catadioptric configuration over the refractive configuration, it seems evident to design reflective cassegrain telescope based optics for the bottom port on LHD. Figure 4 (a) shows the refractive configuration and Fig. 4 (b) shows the catadioptric configurations for location L1 of the infrared camera.

6. Conclusion

The use of an IRVB is very well justified for 3D radiation measurements on LHD and can be successfully used to study the radiation localization in the presence of the magnetic islands. Assuming the foil temperature rise of 5°C and considering the noise equivalent temperature difference of the FLIR SC655 IR camera to be 50 m °C, the signal to noise ratio for the IRVB turns out to be 100. The S_{IRVB} for the new IRVB would approach the theoretical minimum of 44 μW/cm^2 for the SC655 IR camera with the addition of infrared optics which is 5.45 fold better than the S_{IRVB} obtained using a $15^\circ \times 11^\circ$ telephoto lens. The catadioptric cassegrain telescope configuration is chosen

for optics design, considering its robustness against neutrons and high optical throughput.

Acknowledgement

This work is supported by NIFS budget codes NIFS11ULHH026 and NIFS11GGHH001.

[1] B.J. Peterson *et al.*, Plasma Fusion Res. **1**, 45 (2006).
[2] M. Kobayashi *et al.*, Phys. Plasmas **17**, 056111 (2010).
[3] E.A. Drapiko *et al.*, Nucl. Fusion **51**, 073005 (2011).
[4] Y. Feng *et al.*, Contrib. Plasma Phys. **44**, 57 (2004).
[5] D. Reiter *et al.*, Fusion Sci. Technol. **47**, 172 (2005).
[6] B.J. Peterson *et al.*, J. Nucl. Mater. **415**, S1147 (2011).
[7] B.J. Peterson *et al.*, Rev. Sci. Instrum. **72**, 923 (2001).
[8] B.J. Peterson, Rev. Sci. Instrum. **70**, 3696 (2000).
[9] B.J. Peterson *et al.*, Rev. Sci. Instrum. **74**, 2040 (2003).
[10] B.J. Peterson *et al.*, Plasma Fusion Res. **5**, 035 (2010).
[11] B.J. Peterson *et al.*, Plasma Fusion Res. **5**, S2095 (2010).
[12] J. Cantarini *et al.*, Rev. Sci. Instrum. **79**, 10F513 (2008).
[13] S.S. Medley, Rev. Sci. Instrum. **70**, 794 (1999).
[14] S.P. Pandya *et al.*, Plasma Fusion Res. **7**, 2402089 (2012).